Effect of Minor Elements on Fusion Zone Dimensions of Inconel 600

Minor elements, when incorporated into welds by a powder metallurgy insert technique, have significant effects on fusion zone dimensions

BY W. F. SAVAGE, E. F. NIPPES AND G. M. GOODWIN

ABSTRACT. This investigation was undertaken to determine the effect of six minor elements—S, P, Si, Mn, Ti, and Al—on the fusion zone dimensions of Inconel, a solid-solution-strengthened nickel base alloy. A technique was developed which allowed the preparation by welding of a large number of specimens of systematically varied composition by the incorporation of compacted and sintered powder inserts containing the desired "impurity" additions.

A full factorial experiment was performed, utilizing all of the 64 possible combinations of the six intentionally added minor elements. Using the method of Yates and the analysis of variance, the significant effects of the six minor elements were determined for the fusion zone dimensions.

It was found that some of the minor elements had a significant effect on the cross-sectional area and depth of penetration of the GTA weld pads into which the powder inserts had been incorporated. This behavior was postulated to result from the effect of these elements on the anode potential drop.

Introduction

In the production of a direct current, straight polarity (DCSP) GTA weld, the work serves as the anode terminal of the arc, and the size of the weld puddle depends upon the balance between the heat supplied at the anode and the anode heat losses. In a recent article, Ludwig[1] presents a comprehensive summary of these factors.

Considering the forms in which energy is delivered to the anode, as discussed by Ludwig, the mechanisms contributing to anode heating are:

1. The kinetic energy of incident electrons,
2. The thermal energy of incident electrons,
3. The energy delivered to the anode by the conduction of heat by neutral and excited atoms.

Considering the mechanisms by which heat is dissipated from the anode-spot region, the heat losses are a result of:

1. Normal conduction to the surrounding work,
2. Vaporization of material at the anode,
3. Radiation,
4. Melting,
5. Convection,
6. Ion emission at the anode, for positive ions.

Previous work at RPI[2] indicated that the formation of oxides on the surface of a weld puddle could alter the emission of secondary electrons during DCSP GTA welding of Inconel. This would alter the magnitude of the negative space charge in the anode region and cause a change in the anode drop. Thus, a decrease in the anode-drop voltage was postulated to explain the reduction in penetration and cross-sectional area of welds made in cylinder argon contaminated with air.

It is significant to note that, in this previous work at RPI, both the depth of penetration and the cross-sectional area of the weld were observed to change. On the other hand, Ludwig[1] reported, "It has been found that the cross-sectional areas for a given arc power and gas shield, although apparently geometrically different in shape, are independent of anode spot size as long as the depth of melting penetration is not completely through the workpiece thickness." He concluded that the observed variation in penetration was primarily a result of variation in anode spot size brought on by differences in the amount of easily ionized elements, such as Ca, in the base material.

Object

The major objective was the investigation of the influence of six minor elements (S, P, Si, Mn, Ti, and Al), normally present in Inconel 600, on the fusion zone dimensions of DCSP GTA welds.

Materials and Procedure

Preparation of the Basic Ternary Alloy

High-purity (99.9+%) Fe, Cr, and Ni powders were mixed in proportions corresponding to the basic ternary composition of Inconel and consolidated into 4 in. (10.2 cm) diameter rods, 24 in. (61 cm) long, by air induction melting and casting in graphite molds. These rods were then welded together and vacuum consumable arc melted into 6 in. (15.2 cm) molds.

The resulting ingots were then hot

W. F. SAVAGE is Professor of Metallurgical Engineering and Director of Welding Research, and E. F. NIPPES is Professor of Metallurgical Engineering, Rensselaer Polytechnic Institute, Troy, N. Y.; G. M. GOODWIN, former Graduate Research Assistant at RPI, is now with the Metals and Ceramics Division, Oak Ridge National Laboratory, Oak Ridge, Tennessee.

Table 1—Composition of High Purity "Ternary" Base Metal, wt-%

Fe	11.6	Ti	0.02
Cr	15.2	Al	0.03
Ni	72.8	C	0.003
S	0.004	Cu	0.014
P	0.001	H_2	0.0004
Si	0.06	N_2	0.004
Mn	0.064	O_2	0.026

Table 2—High Level Aim Composition After Remelting, wt-%

S	0.015	Mn	1.0
p	0.015	Ti	0.5
Si	0.05	Al	0.5

extruded into sheet bar and rolled into ¼ in. (6.35 mm) plate. The sheet bar was hot rolled initially, followed by cold reduction of 20% to final size.

The basic ternary material was prepared at Oak Ridge National Laboratory and was delivered to Rensselaer in the form of plates, 6 × 6 × ¼ in. (15.2 × 15.2 × 0.63 cm). Table 1 summarizes the chemical composition of these high purity, ternary alloy plates.

Preparation of the Modified Alloy Pads

Since little or no information on the various interactions between the six minor alloying elements (S, P, Si, Mn, Ti, and Al) was available in the literature (except for the proposed Mn + S → MnS reaction[3]), a full-factorial experimental design was chosen—that is, it was elected to investigate the effects of the six elements at two levels of concentration in all possible combinations. Since it was impractical to produce the 64 alloys required by remelting the basic ternary and preparing 64 "split-heats," a unique method was developed for producing the experimental alloys.

Preliminary experiments indicated that the composition of a small

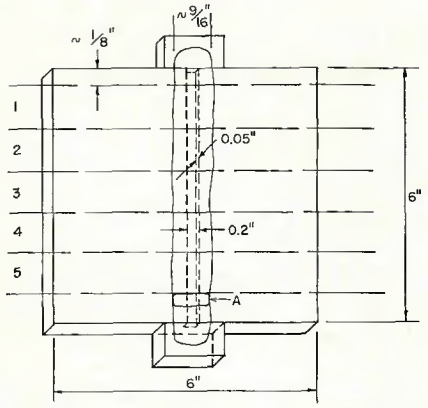

Fig. 1—Schematic representation of sample preparation

volume within each plate of the basic ternary alloy could be modified by the following technique:

1. An alloy insert, prepared by compacting and sintering an appropriate mixture of suitable high purity powders, is inserted in a premachined groove along the centerline of the 6 × 6 in. (15.2 × 15.2 cm) specimens, as indicated by dashed lines in Fig. 1.

2. A series of three wide weave GTA passes (sinusoidal weave pattern with ½ in. (12.7 mm) peak-to-peak oscillation) is then made to melt and mix the insert with an appropriate volume of the basic ternary alloy. Thus, the resulting specimen contains a "pad" of modified composition with a reproducible pattern of microsegregation typical of a weld deposit made under controlled conditions. The solid lines in Fig. 1 represent the typical appearance of a specimen after the GTA remelting operation.

3. Atmospheric contamination is minimized by performing the GTA remelt operation in a high purity argon atmosphere within a laboratory dry box. Contamination by refractory or mold materials is impossible since the entire remelted zone is contained within the basic ternary plate, which thus acts, in effect, as a "crucible."

Table 3—GTA Welding Conditions Used in Inconel Sample Preparation[a]

Welding current	100 A, DCSP
Welding voltage	10 V
Arc gap	3/32 in. (2.38 mm) measured cold
Electrode	1/8 in. (3.2 mm) EWTh2 ground to 90° conical tip
Travel speed	0.9 ipm (22.9 mm/min)
Oscillation	Sinusoidal, amplitude = 0.5 in. (12.7 mm), frequency = 26 oscillations/min
Passes	Three, consecutive, back and forth
Backing plate	Al, water cooled
Hold-down	None
Torch gas	40 CFH (18.9 liters/min) Ar, ionization grade (99.999% minimum)
Power supply	3-phase rectifier

[a]All GTA remelting was performed in a laboratory dry box filled with high purity Ar under a slight positive pressure.

The welding conditions used in preparing the modified alloy pads for subsequent measurement of fusion zone dimensions are summarized in Table 3.

The average cross-sectional area, width and depth of penetration were determined from measurements of several preliminary remelt passes. Based upon these values, an insert geometry of 0.200 × 0.050 × 3.0 in. (5.1 × 1.27 × 76.2 mm) was chosen. With two inserts laid end-to-end in a 6 in. (152.4 mm) long, accommodating groove, an average dilution factor was estimated as follows:

$$\text{Estimated dilution factor} = \frac{\text{volume of insert added}}{\text{avg. total volume remelted}} = 0.08$$

Table 4—Weight % Composition of Typical Inconel Weld Pads

Insert	Fe	Cr	Ni	S	P	Si	Mn	Ti	Al	C	Cu
1	9.63	14.8	74.5	0.005	0.001	0.07	0.056	0.02	0.03	0.003	0.016
11	9.54	14.4	74.7	0.020*	0.001	0.07	0.054	0.31*	0.03	0.003	0.016
19	9.92	14.8	74.5	0.004	0.0005	0.23*	0.050	0.01	0.21*	–	0.01
22	9.23	14.5	75.0	0.004	0.001	0.07	0.060	0.35*	0.33*	0.003	0.014
30	9.34	14.8	74.4	0.016*	0.001	0.15*	0.060	0.23*	0.03	0.002	0.014
39	8.97	14.6	73.4	0.004	0.0008	0.30*	1.200*	0.01	0.21*	–	0.01
53	9.99	14.7	72.3	0.022*	0.010*	0.08	1.400*	0.01	0.27*	–	0.01
56	9.55	14.7	74.6	0.014*	0.004*	0.23*	0.050	0.22*	0.03	–	0.01
64	8.76	14.4	74.5	0.013*	0.004*	0.32*	1.400*	0.37*	0.23*	–	0.01
Avg. without element addition	9.95	14.6	73.7	0.004	0.0013	0.072	0.093	0.014	0.03	0.0028	0.012
Avg. with element addition	9.95	14.6	73.7	0.016	0.0097	0.294	1.331	0.32	0.25	0.0028	0.012

*Element intentionally added.

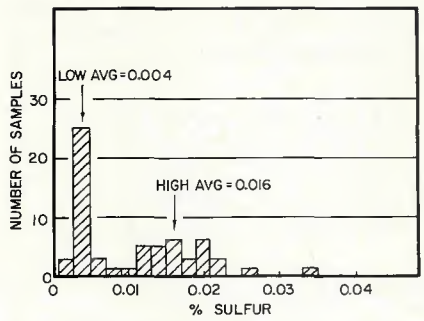

Fig. 2—Distribution of S concentrations in Inconel samples

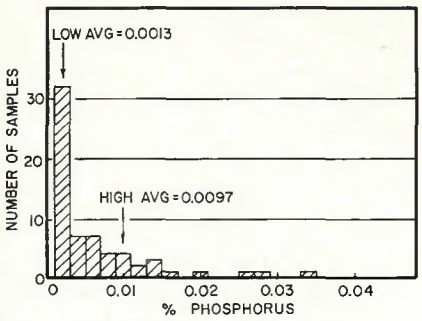

Fig. 3—Distribution of P concentrations in Inconel samples

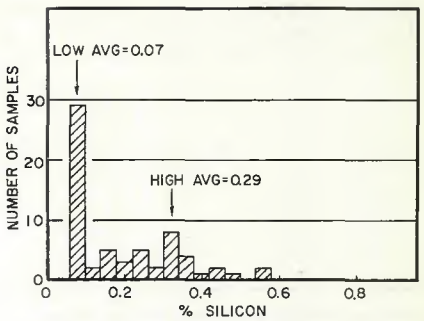

Fig. 4—Distribution of Si concentrations in Inconel samples

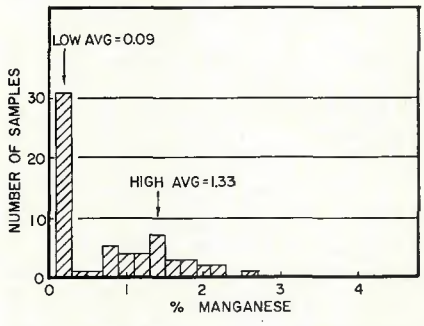

Fig. 5—Distribution of Mn concentrations in Inconel samples

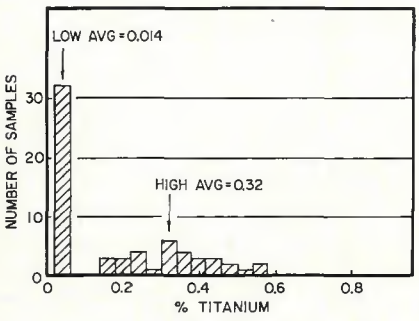

Fig. 6—Distribution of Ti concentrations in Inconel samples

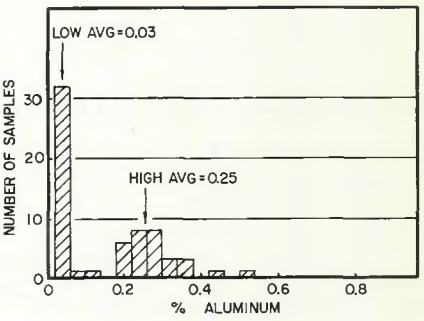

Fig. 7—Distribution of Al concentrations in Inconel samples

Assuming an estimated dilution factor of 0.08, the compositions of the inserts required to produce the aim compositions listed in Table 2 were calculated. These aim compositions represent the approximate upper limits for the six elements in the Inconel specification and were therefore chosen to serve as the "high level" in the factorial experiment. Obviously the "low-level" compositions would therefore correspond to the level of each element present in the basic ternary alloy plates as listed in Table 1.

Insert Preparation

The inserts were prepared from high purity Fe, Cr, Ni, Mn, Ti, and Al powders, with P and S being added in the form of NiP and FeS, respectively. The individual powders making up each insert were weighed to within ±0.001 g, placed in 30 cc vials, and oblique dry blended for one h. The powders were then cold pressed at a pressure of 45 ksi (3165 kg/cm²) using a stearic acid-carbon tetrachloride lubricant. The green compacts were then sintered for 1 h at 1000 C (1832 F) in dry hydrogen, after which they were machined to final size.

Chemical Analysis

The results of the chemical analyses of several typical weld pads are given in Table 4. An asterisk (*) denotes the aim composition of an element. Note, for example, that Insert 1 contains all six factors at their lower levels, Insert 64 contains all six factors at their higher levels, and so on. These compositions may be compared with the desired fusion zone compositions given in Table 2.

Table 5—Cross-Sectional Area and Depth of Penetration of Inconel Weld Pads

Insert	Alloy additions	Area, cm²	Depth, cm	Insert	Alloy additions	Area, cm²	Depth, cm	Insert	Alloy additions	Area, cm²	Depth, cm
1	None	0.445	0.379	23	S-P-Si	0.690	0.485	44	P-Mn-Ti-Al	0.607	0.485
2	S	0.352	0.273	24	S-P-Mn	0.305	0.273	45	P-Si-Ti-Al	0.628	0.564
3	P	0.350	0.291	25	S-P-Ti	0.543	0.431	46	P-Si-Mn-Al	0.740	0.458
4	Si	0.616	0.475	26	S-P-Al	0.347	0.273	47	P-Si-Mn-Ti	0.717	0.635
5	Mn	0.552	0.467	27	S-Si-Mn	0.520	0.405	48	S-Mn-Ti-Al	0.400	0.255
6	Ti	0.758	0.635	28	S-Mn-Ti	0.498	0.387	49	S-Si-Ti-Al	0.520	0.361
7	Al	0.458	0.344	29	S-Ti-Al	0.395	0.291	50	S-Si-Mn-Al	0.542	0.387
8	S-P	0.515	0.378	30	S-Si-Ti	0.591	0.493	51	S-Si-Mn-Ti	0.732	0.635
9	S-Si	0.605	0.502	31	S-Si-Al	0.578	0.546	52	S-P-Ti-Al	0.520	0.440
10	S-Mn	0.398	0.317	32	S-Mn-Al	0.535	0.405	53	S-P-Mn-Al	0.430	0.326
11	S-Ti	0.601	0.493	33	P-Si-Mn	0.525	0.415	54	S-P-Mn-Ti	0.513	0.458
12	S-Al	0.402	0.344	34	Si-Mn-Ti	0.637	0.493	55	S-P-Si-Al	0.605	0.387
13	P-Si	0.635	0.510	35	P-Mn-Ti	0.815	0.635	56	S-P-Si-Ti	0.900	0.635
14	P-Mn	0.505	0.422	36	P-Si-Ti	0.757	0.635	57	S-P-Si-Mn	0.783	0.635
15	P-Ti	0.775	0.635	37	P-Mn-Al	0.673	0.635	58	P-Si-Mn-Ti-Al	0.593	0.370
16	P-Al	0.373	0.273	38	P-Si-Al	0.511	0.387	59	S-Si-Mn-Ti-Al	0.719	0.546
17	Si-Mn	0.575	0.537	39	Si-Mn-Al	0.512	0.431	60	S-P-Mn-Ti-Al	0.395	0.282
18	Si-Ti	0.483	0.387	40	P-Ti-Al	0.493	0.361	61	S-P-Si-Ti-Al	0.725	0.635
19	Si-Al	0.633	0.635	41	Si-Ti-Al	0.581	0.520	62	S-P-Si-Mn-Al	0.635	0.449
20	Mn-Ti	0.685	0.546	42	Mn-Ti-Al	0.435	0.273	63	S-P-Si-Mn-Ti	0.779	0.635
21	Mn-Al	0.452	0.387	43	Si-Mn-Ti-Al	0.535	0.326	64	S-P-Si-Mn-Ti-Al	0.706	0.635
22	Ti-Al	0.302	0.291								

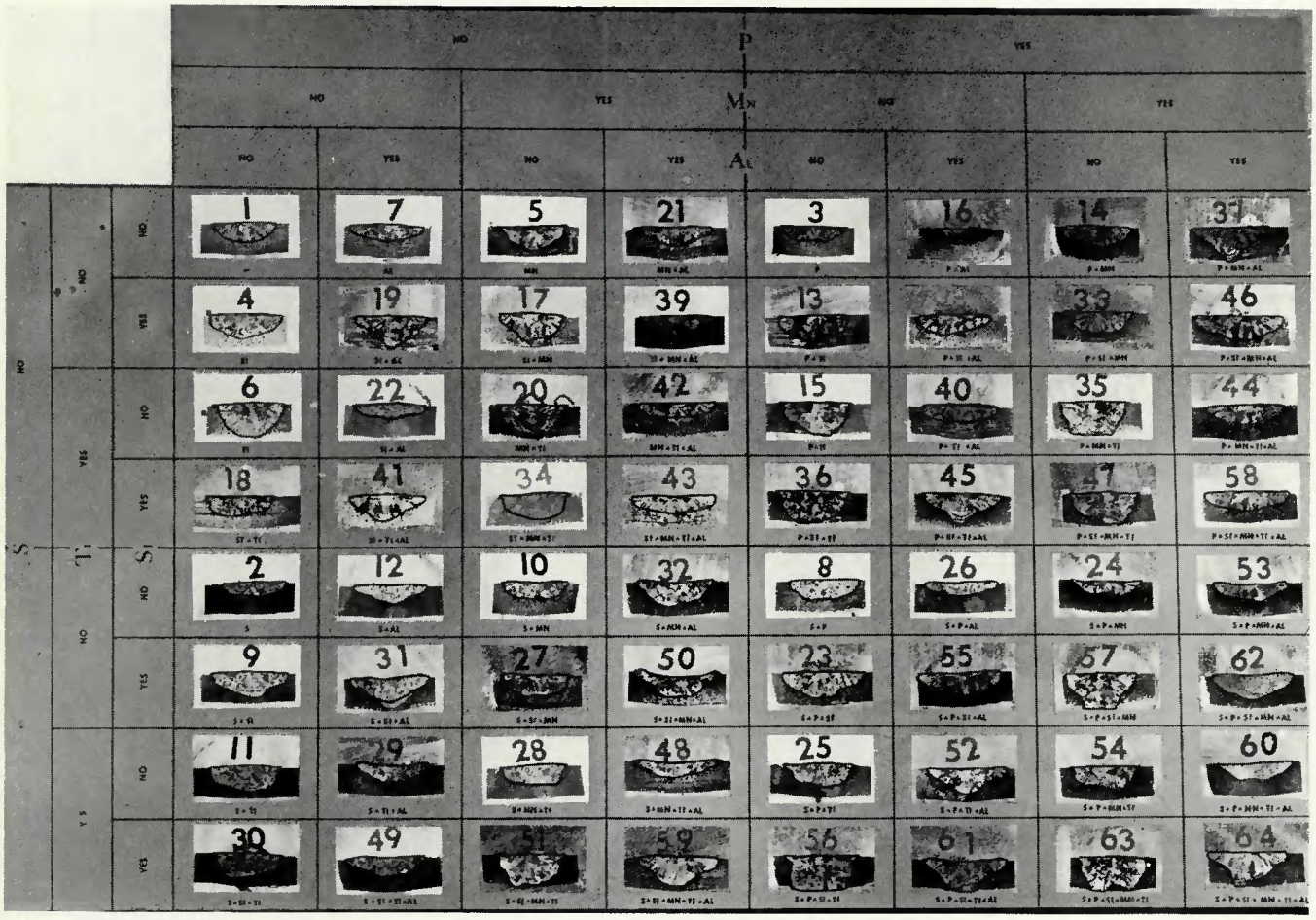

Fig. 8—Cross-sections of Inconel weld pads

The significance of the analyses is best seen by looking at the distribution of compositions obtained; Figs 2–7 show these distributions. Figure 2 is a histogram showing the frequency of occurrence of a particular S concentration as a function of %S. Ideally, this distribution would show one half (32) of the samples at 0% and the other half at the desired nominal composition, 0.015%S.

Obviously, this cannot be attained in actual practice, since trace amounts of the element are always present even in the "purest" base material, and there must be some distribution of actual compositions about the design nominal. Several factors contribute to this distribution, including human error in preparing the powder inserts, inhomogeneous distribution of the impurity elements in the fusion zone, losses of impurity elements during the welding process, inaccuracy in measurement of the actual composition, and variations in the volume of the base ternary remelted with inserts of various compositions.

The average high level of S concentration was then found by taking the average S content of those samples to which S was intentionally added. Similarly, the average lower level of S content is determined from those samples to which S was not intentionally added. These calculated average compositions are listed at the bottom of Table 4 and are also shown in Figs. 2–7.

The transverse sections removed from each of the 6 × 6 in. (15.2 × 15.2 cm) plates (section A, Fig. 1) were mounted, polished and etched for metallographic examination. Photomacrographs were taken and enlarged to ×4, and the depth of penetration and cross-sectional area measurements were made from these photographs. Cross-sectional area was measured using a polar planimeter, averaging the results of three readings, and the penetration was measured with a scale.

A composite photograph, showing each of the individual transverse sections is shown in Fig. 8. The numbers on the cross-sections refer to insert numbers, as given in Table 5, which lists the alloy additions, cross-sectional area, and depth of penetration for all 64 weld pads. Note that the photographs are arranged systematically; for example, the last four columns all have P present as an intentional addition, while the first four do not. Each of the other "impurity" elements are arranged in the composite as indicated by the headings, and as shown under each individual transverse section.

Results

The effects discussed here were determined by application of the method of Yates, and the significance of these effects was estimated by the analysis of variance[4-6]. For both the cross-sectional area and the depth-of-penetration parameters, the individual responses, effects, and sums of squares for each of the 64 possible treatment combinations were determined, along with an analysis of variance.

This section considers only those effects determined to be significant at the $\alpha = 0.1\%$ and 0.5% levels for these two parameters.

Cross-Sectional Area

For the case of the cross-sectional area of the weld pad, the response which was considered was the % change in cross-sectional area of a particular specimen as compared with that of a specimen containing all factors at their lower level (Insert 1). Stated mathematically:

$$R_A = (100A/A_o) - 100$$

where R_A is the response, A_o is the

Table 6—Summary of Results: Cross-Sectional Area of Weld Pads

Treatment combination	Effect	α, %	Best value
Si	31.3	0.1	17.3
Ti	18.1	0.1	37.9
S-Si	17.7	0.1	35.0
Ti-Al	−16.2	0.5	6.4
Al	−15.4	0.5	4.4
P	14.1	0.5	17.7
Mean	—	—	27

cross-sectional area of the specimen containing the lower level of all factors, and A is the cross-sectional area of the specimen being considered. Note that the response may be either positive or negative—(+) indicating an increase in area, and (−) indicating a decrease in area.

Because the cross-sectional area determinations, which are presented in Table 5, were not replicated, the analysis of variance was conducted by assuming that all 5 and 6 factor interactions were negligible. Thus, the estimate of error mean square was based upon seven comparisons, *i.e.*, the six 5 factor interactions and the single 6 factor interaction.

The significant effects which were determined are shown in Table 6. Note that Table 6 lists the effects in decreasing order, beginning with the largest and therefore most significant effect. Also shown in Table 6 are the significance levels (α values) and the calculated best value for each of the treatment combinations shown.

Note that the first three effects are significant at the $\alpha = 0.1\%$ level and the last three at the 0.5% level. It was decided not to include any further effects, since the seventh highest significant effect, Si-Ti-Al, was only significant at the $\alpha = 5\%$ level, a considerable jump from the 0.5% level.

The magnitude and sign of the individual effects are also shown graphically in Fig. 9. Note from Fig. 9, and from Table 6, that Si has by far the strongest overall effect on cross-sectional area of the weld pad. The positive effect of Si indicates that the average cross-sectional area of the 32 samples containing Si as an intentional addition is greater than the average cross-sectional area of the 32 samples in which Si was not added intentionally, *i.e.*, the addition of Si increases cross-sectional area, on the average.

However, the best value, which was calculated for the specimens containing only Si as an impurity element, is only a 17.3% increase in area, compared with an average for all specimens of a 27% increase in area. For this to be possible, the effect of Si must be greater when others of the impurity elements are present than it is when Si alone is present as an intentionally added impurity element. It will later be seen that this is indeed the case.

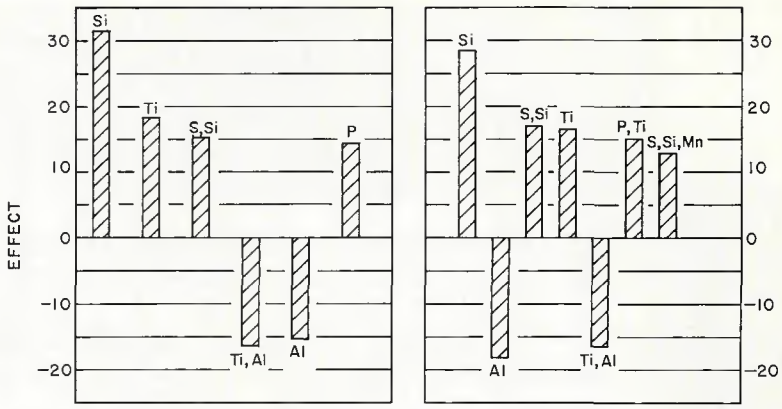

Fig. 9—Summary of effects on cross-sectional area and depth of penetration: left—cross-sectional area; right—depth of penetration

The second strongest effect is Ti, also a positive effect, but only roughly one-half as strong as the effect of Si (18 vs. 31). The best value for the specimen containing only Ti as an intentional addition is 37.9, a value considerably greater than the mean. From this we can see that Ti is effective at increasing the cross-sectional area when it is present alone, as well as in the presence of other elements.

The positive S-Si interaction indicates that the effect of Si is greater when S is present than when S is absent. Thus, the S-Si interaction explains why the best value for the specimens containing only Si was low, since Si is considerably more effective at increasing cross-sectional area when S is also present.

The fourth significant effect is a negative Ti-Al interaction, indicating that the effect of Ti is decreased by the presence of Al. The interaction is especially strong for the specimens containing only Ti and Al, as witnessed by the low best value for the Ti-Al treatment combination.

The fifth significant effect is a negative effect for Al, indicating that, in general, Al decreases the cross-sectional area of the weld pad.

Table 7—Summary of Results: Depth of Penetration of Weld Pads

Treatment combination	Effect	α, %	Best value
Si	28.4	0.1	31.4
Al	−18.1	0.1	5.5
S-Si	17.0	0.1	35.5
Ti	16.6	0.1	25.1
Ti-Al	−16.5	0.1	−9.6
P-Ti	15.1	0.5	19.2
S-Si-Mn	12.9	0.5	48.4
Mean	—	-	19.2

Although none of the best values shown in the summary table is negative, there are treatment combinations which will result in negative best values, i.e., combinations which will have cross-sectional areas lower than that of the "pure" ternary.

The final effect significant at the $\alpha = 0.5\%$ level is a positive effect of P, indicating that P additions tend to increase the average cross-sectional area. As indicated by the fact that the best value for the P-treatment combination is less than the mean, this effect is stronger when other elements are also present as intentional additions.

Depth of Penetration

The response which was considered for the depth of penetration data was the % change in depth of penetration for a given specimen as compared with the specimen containing all factors at their lower level (Insert 1). Thus:

$$R_d = (100d/d_o) - 100$$

where R_d is the response, d is the penetration, and d_o is the penetration for the specimen containing Insert 1. It should be noted that this response has an upper limit of 68% when full penetration is achieved. As was the case with the response for cross-sectional area, this response may be either positive or negative.

The depth of penetration data are presented in Table 5. A summary of the significant effects on depth of penetration is given in Table 7, and these effects are shown graphically in Fig. 9.

There are five effects on penetration which are significant at the $\alpha = 0.1\%$ level, and two effects significant at the $\alpha = 0.5\%$ level, indicating that penetration is a slightly more sensitive indicator than is cross-sectional area.

The first five significant effects on depth of penetration are the same as the first five effects on cross-sectional area, the only difference being the order in which these effects occur.

This might have been expected, since the width of the weave bead was controlled primarily by the lateral width of the mechanical oscillation which was employed in the production of the weld pad. Only a slight amount of variation in the width of the weld pad was possible, and therefore penetration should be the most important factor influencing the cross-sectional area.

Silicon again had the strongest overall effect, again by a considerable margin. In this case, note that the best value for the Si-treatment combination is considerably above the mean, indicating that even Si alone is quite effective at increasing the depth of penetration.

The second most signficant effect is that of Al. Note that Al tends to decrease the depth of penetration just as it decreased the cross-sectional area, but that the effect is more significant on depth of penetration than on cross-sectional area.

The third strongest effect is the S-Si interaction. This effect is of the same sign and nearly the same magnitude as that for the cross-sectional area, indicating once again that Si is considerably more effective at increasing the depth of penetration when S is also present. Note that the best value is considerably above the mean.

Titanium has the fourth strongest effect, again positive. The best value for the Ti-treatment combination is above the mean, indicating that Ti has a strong influence even in the absence of the other "impurity" elements, as was the case in the cross-sectional area analysis.

The fifth effect is a negative Ti-Al interaction. As discussed for the case of the cross-sectional area, this interaction indicates that the presence of Al inhibits the effect of Ti; in this case, in fact, Al completely dominates, and the best value for penetration is less than that of the "pure" ternary material.

The sixth strongest effect is a positive P-Ti interaction, indicating that on the average, P enhances the effect of Ti. This enhancement occurs primarily when other "impurity" elements are present, as evidenced by the fact that the best value for the P-Ti treatment combination is the same as the mean.

The last effect significant at the $\alpha = 0.5\%$ level is a 3 factor interaction, S-Si-Mn. This result indicates that the effect of Si is enhanced by the presence of S, as was indicated previously, but especially so in the presence of Mn. Note that the best value for this treatment combination is very large. The presence of this third-order effect emphasizes the strength of the Si and S-Si effects.

Discussion of Results

The surprisingly large influence of minor element concentration on penetration characteristics was completely unexpected. The practical implications of this observation are obviously great, since all concentrations of the elements added are within the tolerances of the Inconel 600 specification. Thus, significant variations in penetration, often attributed to inadequate control of welding variables in semi-automated GTA welding processes, may well arise from base metal compositional variations from lot to lot.

In the present case, no "readily ionized" elements fitting Ludwig's description[1] were added, and no contact with Ca-containing refractories was possible during either the production or the remelting of the basic ternary. Furthermore, both the depth of penetration and the cross-sectional area showed similar types of response to the intentional additions. Thus, it is most probable that the mechanism or mechanisms involved are more complex than Ludwig's model would suggest.

The most likely manner in which minor elements could affect the penetration characteristics of a weld is through a change in the anode potential drop, E_a.[7,8] It is important to note that the major contribution to anode heating is due to the kinetic energy of incident electrons. This energy is distributed over a distance of one mean free path from the work surface and is dissipated by collision with the work surface. The plasma power is dissipated largely by radiation and convection, and the cathode power is represented by the thermal and kinetic energy of electrons leaving the cathode. This energy is subsequently dissipated in the plasma region. Thus, neither the cathode power nor the plasma power have a direct effect upon anode heating except through radiation and transfer of thermal energy from those particles which strike the work.

Increasing the amount of secondary electron emission from the anode surface increases the anode potential drop, E_a. This may be visualized as follows: incident electrons having sufficient energy to overcome the work function will cause emission of one or more secondary electrons from the anode surface. Since the energy of these secondary electrons is of necessity quite low (in the order of a few electron volts), the distribution of secondary electrons would be expected to form a negative space charge in the vicinity of the anode-drop region. The presence of a negative space charge causes an increase in the potential gradient in the anode region, i.e., an increase in the anode potential drop. Since the kinetic energy of incident electrons is essentially determined by the potential through which the electrons fall during their last mean free path and is transferred to the anode by direct collision, it is clear that the anode potential drop, E_a, is a critical factor in determining the melting efficiency of the arc.

However, the anode power density is dependent upon the anode spot size, and thus any factor which tends to constrict the anode-spot size without changing total power, would, as Ludwig suggests, alter the penetration.

It should be reemphasized that in this experiment both the cross-sectional area and the depth of penetration were affected by some of the intentional impurity additions; thus, from the above argument, the anode potential drop must have been altered, since constriction of the anode spot size alone cannot account for the observed change in cross-sectional area.

Quite possibly both effects are operative, but unfortunately the determination of the effective diameter of the anode surface in this experiment was precluded by the use of a mechanically oscillated weave bead.

The production and release of positive ions at the anode, as suggested by Ludwig, are not necessary to account for the change in anode potential drop. However, elements having a low ionization potential would also tend to exhibit greater secondary electron emissivity, and conversely. Thus, those elements which are easily ionized, such as Ca, would also be expected to have a strong effect on E_a.

It is difficult to obtain from the literature reliable estimates of the work function and the secondary electron emission ratio, δ (the maximum number of secondary electrons emitted per primary electron) for the elements intentionally added in this experiment. Almost no information was available for S, P, or Mn; the data which were available[9,10] are summarized as follows:

1. Silicon, which increased both penetration and cross-sectional area, has approximately the same work function, both as in elemental form and when present as the oxide, SiO_2. (4.8 eV. vs. 5.0 eV., respectively.) The secondary electron emission ratio, δ, however is quite high for the oxide, $\delta = 2.1$ to 4.0, indicating that Si could increase the anode potential drop through an increase in electron emission from its oxide, SiO_2. (For each of the elements considered, the secondary electron emission ratio for the elemental form was approximately unity.)

2. Titanium, another element which increased penetration and cross-sectional area, has a higher work function for the elemental form than for the oxide, TiO, 3.95 eV vs. 3.0 eV., respectively. Although no definite information was available in the literature concerning the secondary electron emission ratio of TiO, it is expected that the value is high, since rutile, TiO_2, is purposely added to welding electrodes to increase emissivity and stabilize the arc.

3. Aluminum, which decreased penetration, has a high secondary emission ratio for its oxide, Al_2O_3, (2.0-9) but the oxide also has a high work function compared with the elemental form, 4.7 eV. vs. 4.25 eV., respectively. It should be noted that the emission ratios which are quoted here are the maximum ratios which invariably occur at higher energies than those involved in this type of arc phenomenon, and thus the work function is probably of more significance in this instance. In any case, it is expected that the overwhelming effect of Al is a result of the shielding effect of the refractory oxide layer formed during the production of the weld.

It is important to note that the large amount of scatter in both the cross-sectional area and the depth of penetration from the calculated best values precludes the drawing of precise conclusions as to the effect of various elements on these parameters from the observation of individual specimens. In the majority of cases, the agreement between experimental values and calculated best values was good; however, whenever high degrees of scatter are involved, one cannot eliminate the possibility of a completely atypical result.

For example, the calculated best value for the cross-sectional area of the sample containing Insert 3 (P addition), was highly atypical. The best value was an increase in area of 17.7% over the area of the basic ternary specimen containing Insert 1. Measurements made from the sample containing Insert 3 show a decrease in area of 21% from the area of the specimen containing Insert 1. However, the best value and observed value of penetration, −9 and −23, respectively, are in somewhat better agreement for this element.

Several factors probably contribute to this observed variation. Additional transverse sections were cut from some of the specimens, and it was noted that the measured cross-sectional area in extreme cases varied by more than 20% within a distance along the weld centerline of only ½ in. (12.7 mm). This effect is most probably a result of a variation in the degree to which the specimen contacted the water-cooled Al backing plate (recall that the specimens were not mechanically restrained during the GTA remelting of the weld pad).

It is also possible that there is a significant variation in the cross-section of the weld pad from one end to the other of the 6 × 6 × ¼ in. (15.2 × 15.2 × 0.63 cm) plate. Since three weld passes were used to produce the weld pad, perhaps the "terminal" end of the weld pad would have a consistently different cross-section than the "starting" end, as a result of a difference in the thermal histories of these two locations. For the purposes of this experiment, the transverse sections were taken from either end of the weld pad at random to eliminate the effect of any such variation on the final results.

CONCLUSION

1. It was found that the composition of Inconel 600 samples could be altered and controlled within reasonable limits by the introduction of powder inserts containing the desired additions and using a series of wide weave GTA passes to melt and mix the minor additions with the base metal.

2. With regard to the penetration characteristics of the remelted weld pad on Inconel 600:
(a) Si and Ti strongly increased both the cross-sectional area and depth of penetration of the weld pad, presumably as a result of a change in the anode potential drop.
(b) The effect of Si was increased by the presence of S, and the effect of Ti was decreased by the presence of Al.
(c) P increased the cross-sectional area of the weld pad, probably by the same mechanism as Si and Ti.
(d) Al decreased both the cross-sectional area and depth of penetration of the weld pad, probably as a result of the formation of a refractory-oxide layer on the surface of the weld puddle.

References

1. Ludwig, H. C., "Current Density and Anode Spot Size in the Gas Tungsten Arc," *Welding Journal*, 47 (5), May 1968, Research Suppl., pp. 234-s to 240-s.

2. Savage, W. F., Lundin, C. D., and Goodwin, G. M., "An Effect of Shielding Gas on Penetration in Inconel Weldments," Technical Note, *Welding Journal*, 47 (7) July 1968, Research Suppl., pp. 313-s and 322-s.

3. Kaubausen, E., "Welding of Austenitic Steels for High Pressure Boiler Plants," *Proceedings of the World Metallurgical Congress*, American Society for Metals Publication, (1951).

4. Davies, O. L., *The Design and Analysis of Industrial Experiments*, Hafner Publishing Company, N. Y., N. Y., (1960).

5. Cochran, W. G., and Cox, G. M., *Experimental Designs*, John Wiley & Sons, Inc., N. Y., N. Y., (1957).

6. Bowker, A. H., and Lieberman, G. J., *Engineering Statistics*, Prentice-Hall, Inc., Englewood Cliffs, New Jersey, (1959).

7. Savage, W. F., and Chase, T. F., Jr., "The Effects of Anode Composition on Tungsten Arc Characteristics," *Welding Journal*, 50 (11), Nov. 1971, Research Suppl., pp. 467-s to 473-s.

8. Savage, W. F., Nippes, E. F., and Chase, T. F., Jr., "Effect of Anode Composition on Potential Distribution in Gas-Tungsten Arcs," *Welding Journal*, to be published.

9. *Handbook of Chemistry and Physics*, 49th Edition, The Chemical Rubber Publishing Company, Cleveland, Ohio, 1968.

10. Fomenko, V. S., *Handbook of Thermionic Properties*, Authorized Translation, Plenum Press Data Division, N. Y., N. Y., (1966).